Experimental Investigation of Cavitation Influence on Hydroacoustic Resonance in Pipe

Nicolas Ruchonnet[*]

Laboratory of Hydraulic Machines, EPFL Lausanne, Switzerland

Christophe Nicolet

Power Vision Engineering sàrl, Ecublens, Switzerland

Sébastien Alligné

Laboratory of Hydraulic Machines, EPFL Lausanne, Switzerland

François Avellan

Laboratory of Hydraulic Machines, EPFL Lausanne, Switzerland

P1

ABSTRACT

At part load operation of Francis turbine, the swirl in the draft tube leads to flow instability known as vortex breakdown. This flow instability can interact with the rest of the hydraulic circuit through axially propagating plane-waves. Moreover, at low cavitation index σ, the gaseous rope is suspected to modify locally the propagation velocity. Hydroacoustic models have been commonly used to tackle this problematic. In order to validate the parameters of those models, an experiment with equivalent phenomenology has been setup. The experiment is designed in order to distinguish the flow instability and its interaction with the acoustic field. The hydraulic circuit consists in a square pipe connecting two constant pressure reservoirs. The excitation mechanism is obtained by the shedding of vortices in the wake of a bluff body placed at ¾ of the pipe length. To examine the influence of the vapour cavity formed in the wake of the bluff body, the mean pressure inside the pipe is adjustable. The excitation mechanism and pipe response have been studied with and without cavitation. The influence of the cavitation index on the resonance frequency and amplitude has been analysed. A strong influence of the cavitation index on the resonant amplitude is shown.

KEYWORDS

Hydroacoustic, resonance, cavitation.

[*] *Corresponding author:* Laboratoire des machines hydrauliques, av. de cour 33bis, CH-1007 Lausanne, Switzerland, phone: +41 21693 25 08, fax: +41 21693 35 54, email: nicolas.ruchonnet@epfl.ch

1. INTRODUCTION

During the exploitation of Francis turbine, flow instability in the draft tube may lead to pressure oscillation inducing unacceptable pressure fluctuation or even power swing. This phenomenon, known as surge, can in the worst cases damage the mechanical components of the installation [1]. At part load operation, the velocity triangle is modified in such a way that a co-rotating peripheral component of velocity remains at the outlet of the runner. The resulting swirl leads to flow instability in the draft tube known as vortex breakdown. This flow is characterized by a dead zone at the centre of the draft tube and a helicoidal vortex precessing at 0.2 to 0.4 times the runner speed. This local instability can interact with the rest of the hydraulic circuit through planar wave propagation. For this reason, acoustic resonance is of major importance in the study of the dynamic stability of Francis turbine. The study of pressure fluctuation generated hydrodynamically begins with the pioneer work of Lighthill [2], [3], [4] and is still a popular domain of research. The common approach is to split the problem in two parts. The source region where fluctuations are generated hydrodynamically and the far field where fluctuations are propagating as pressure waves. Three types of source are distinguished. The monopole source is associated with the variation of density; the dipole source is associated with a fluctuating force on a material surface and the quadrupole source with the free stream turbulence. Specific application to pipe flow is more seldom [5] and is mainly focused on turbulence noise. In the 80's, Dorfler applied the theory of hydroacoustic to Francis turbine [6]. The part load surge is interpreted as the coincidence of the vortex breakdown frequency with one Eigen frequency of the entire circuit. The other key element of the part load surge is the modification of the compliance in the draft tube by the cavitating vortex: following Brennen's definition [7], the variation of vapour volume is function of the pressure variation, Eq.(1).

$$C_V = -\rho \, \partial V \big/ \partial p \qquad (1)$$

The parameter C_V is assumed to be a function of the cavitation index. As a result, the cavitation index modifies the Eigen frequency of the system. Based on this approach, the part load surge occurs as the dipole source frequency matches the modified Eigen frequency of the system. Additionally, it has been pointed out that the distributed model of compliance is equivalent to a distribution of modified propagation velocity along the draft tube [8] and [9].

This paper presents experimental results on a case study featuring same general behaviour but with a high level of simplification. A hydrodynamic source of fluctuation with vapour cavity interacts with a mono dimensional hydraulic circuit. As the fluctuation frequency is low, planar wave propagation is assumed in the pipe. Given the pipe cross section, the cut off frequency is equal to ~2500 Hz, see [10]. The experiment setup consists in a square pipe connecting two constant pressure reservoirs. Due to the large capacity of the reservoirs, the impedances at the pipe boundaries are close to zero for a large band of frequency. The dipole source is obtained by the shedding of vortices in the wake of a bluff body. This type of flow has been extensively studied; see Wille [11] and Williamson [12]. The alternate nature of the flow instability gives rise to a fluctuating pressure acting on the body surface with a frequency proportional to the flow velocity. The resulting lift and drag forces show similar nature. More precisely, the lift frequency is equal to the vortex shedding frequency and the drag frequency is twice the shedding frequency which is proportional to the flow velocity through Eq. (2).

$$St = \frac{f_{lift} D}{C} \qquad (2)$$

To control the volume of vapour in the wake of the bluff body, the pressure inside the pipe is adjusted with a vacuum pump. Finally, pressure sensors have been placed near the bluff body to monitor the hydrodynamic instability and along the pipe to determine the resulting acoustic pressure field. In a first step, the linear relation between the flow velocity and dipole source frequency is verified. Additionally the Eigen frequency of the pipe without cavitation is determined. Then, the influence of the cavitation index is tested. It is observed that the vapour cavity increases the level of fluctuations. The pulsation of vapour volume is suspected to act as a monopole source located downstream the bluff body [13]. The spectral analysis of the acoustic field highlights the influence of the vapour compliance on the Eigen frequencies and mode shapes. With vapour cavity, the resonance frequency and amplitude becomes a function of the cavitation index. The maximum amplitude is reached as the excitation frequency matches the 2nd Eigen frequency and in this case the measured fluctuations are much higher than without cavitation.

2. EXPERIMENTAL SETUP

The experimental setup consists in a pipe connecting two constant pressure reservoirs. A vertical cut of the installation is displayed in Fig. 1. The pipe with a total length of 1.05 m is of square cross section, 0.04 by 0.04 m. The wall thickness is equal to 0.02 m, it is made of PVC. The bluff body is mounted on a Plexiglas support placed at ¾ of the pipe length, see Fig. 2. The shape of the bluff body is semi circular. The rounded face is mounted upstream and the flat surface downstream. Its diameter D is equal to 0.02 m for a length of 0.04 m, the corresponding blockage ratio is equal to ½.
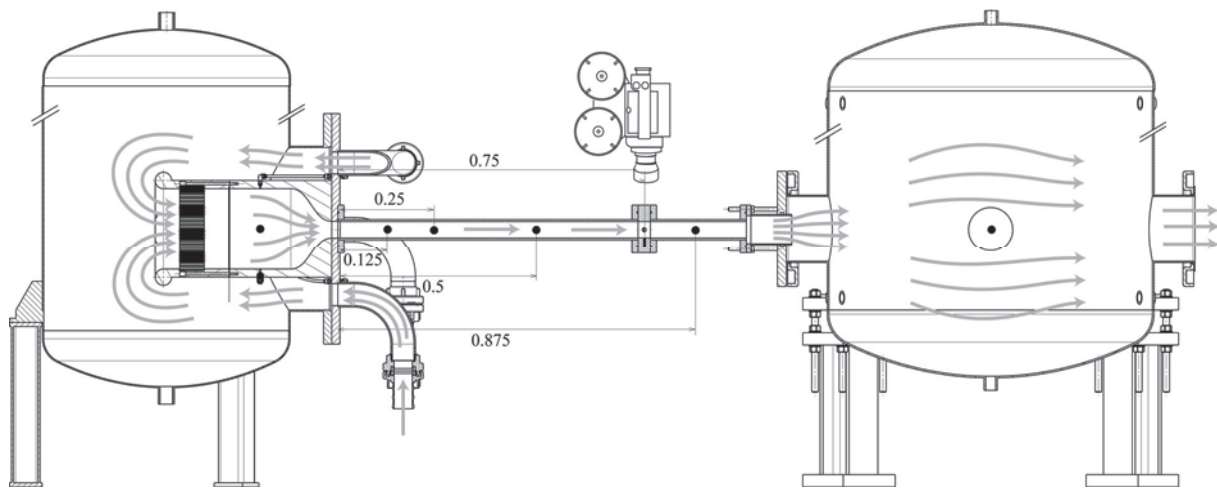
P1

Fig. 1: Vertical cut of the experiment; the flow is from left to right. The bluff body is situated at 0.75 m from the inlet, details in Fig. 2. The pressure sensors are placed at 0.125, 0.25, 0.5, 0.75, 0.875 m from the inlet. Additional pressure sensors are located in the reservoirs. High speed camera is placed above the bluff body.

The operating parameters are the mean velocity C in the pipe and the cavitation index σ, Eq.(3).

$$\sigma = \frac{p - p_v}{1/2 \, \rho C^2} \tag{3}$$

p is the pressure below the bluff body; p_v is the vapour pressure, p_v=2338 Pa for water at 20°C and C is the flow velocity in the pipe. The water circulation is guaranteed by a variable speed pump of 3.3 KW connected in parallel to the reservoirs, the flow velocity can be adjusted from 0 to 10 m/s. The cavitation index is adjusted with the help of a vacuum pump connected

to the downstream part of the circuit. In order to have a stable flow in the pipe, the upstream reservoir is equipped with a convergent (1/25 cross section ratio). At the pipe inlet, the flow goes first through a honeycomb (5 mm hexagon mesh) and a screen (10 mm holes for 0.25 open area ratio) before being accelerated in the convergent. With this assembly, a stable inflow with homogenous turbulence level is guaranteed.
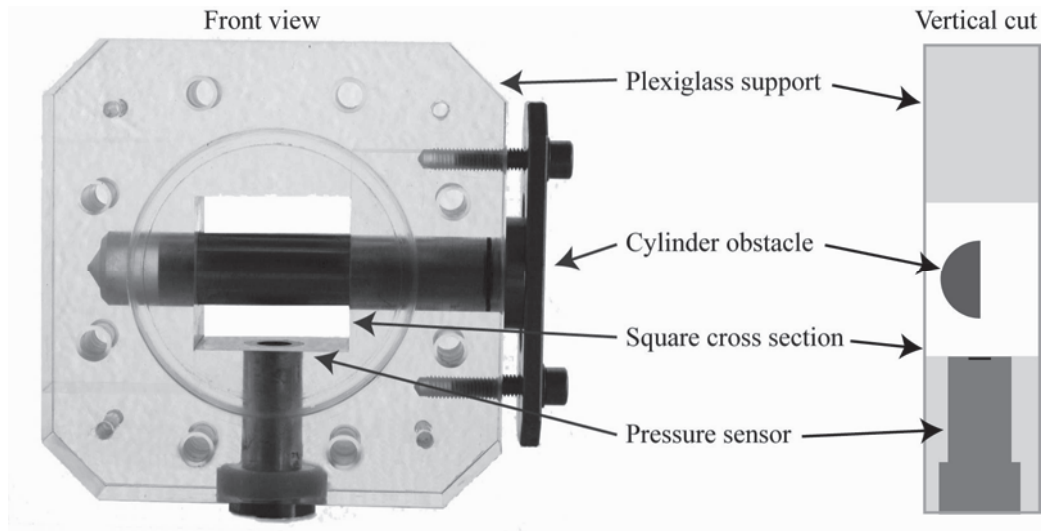

Fig. 2: Plexiglas support with semi circular cylinder bluff body. The pressure sensor is flush mounted below the mid-span bluff body's trailing edge.

The flow rate is monitored with a vortex flow meter of range 0-70 m^3/h placed between the pump and the upstream reservoir. To achieve the monitoring of pressure fluctuation, piezoresistive sensors are distributed along the test region. The sensors are calibrated for absolute pressure ranging from 0.2 to 1.8 bar. The dynamic response has been validated in previous experimentation by Farhat and al. [15]. The sensors are placed at 0.125, 0.25, 0.5, 0.875 m from the pipe inlet, see Fig. 1. One additional sensor is flush mounted in the Plexiglas support below the bluff body, see Fig. 2. This sensor is used for the determination of the vortex shedding frequency. Finally, pressure measurement is also performed in the upstream and downstream reservoir in order to validate the hypothesis of constant pressure.
After amplification, all signals are digitalized synchronously with a NI DAQ6221 at a frequency of 1000 [Hz] and stored directly on a PC. For spectral analysis, Welch's method is used; the parameters are given in Tab. 1:

Sampling frequency	1000 Hz
Time signal duration	66 s
Window size	2^{10} samples
Windows overlap	2^8 samples
Window type	Hamming

Tab. 1: Welch's method parameters.

The visualization of the vapour cavity in the wake of the bluff body is performed with a high speed camera. The CCD image resolution is equal to 640x512 pixels for an acquisition rate of 3000 frames/sec with an exposure time of 80 μs.

3. RESULTS WITHOUT CAVITATION

Hydrodynamic source

For the case without cavitation, the principal hydrodynamic source is the vortex shedding in the wake of the bluff body. From a hydroacoustic point of view, this complex flow phenomenon can be approximated as a dipole source located at the bluff body position [16]. To characterize this source, the sensor located near the bluff body has been used, see Fig. 2. The hydrodynamic instability is characterized by a periodic fluctuation with a variable low frequency modulation see Fig. 3. Its mean amplitude and frequency vary with the flow velocity.

P1
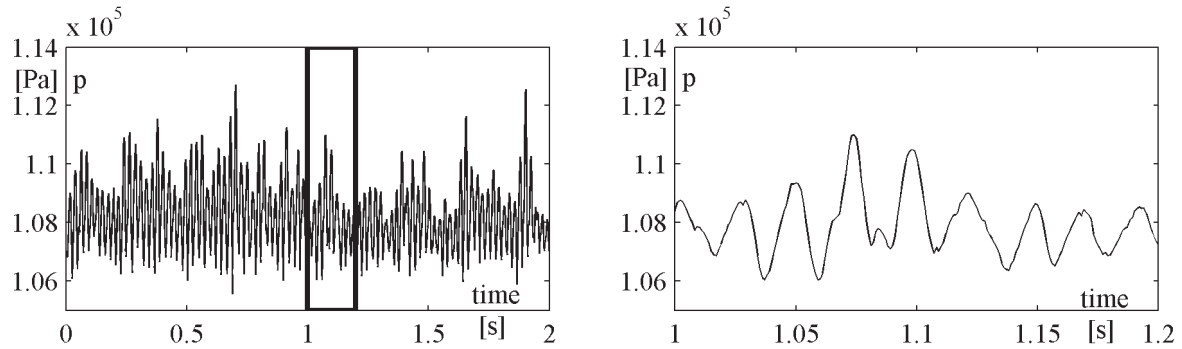
Fig. 3: Absolute pressure below the bluff body for a flow velocity of 2.3 m/s

The pressure sensor is placed at the vertical of the bluff body. For this reason, the fluctuations are proportional to the vortex shedding frequency. And as predicted by relation (2), the vortex shedding frequency is proportional to the flow velocity. Using linear regression, see Fig. 4, the Strouhal number is calculated in Eq 4. This unusual value is due to the high aspect ratio between the pipe and the bluff body cross section; see [14].

$$St = \frac{f_{lift}D}{C} = 0.39 \tag{4}$$

As the source direction inducing planar waves is parallel to the pipe axis, the dipole source is driven by the drag force. For this reason, the dipole source frequency is equal to twice the vortex shedding frequency, see Eq 5.

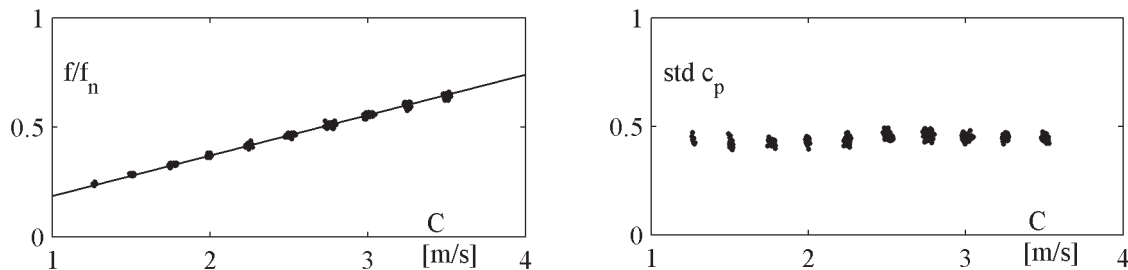$$f_s = f_{drag} = 2f_{lift} = \frac{2St}{D}C \tag{5}$$

Fig. 4: Left: Lift frequency as a function of the flow velocity; points: measure, line: linear regression. Right: Standard deviation of the pressure coefficient below the bluff body as a function of the flow velocity.

In order to validate the relation between the dipole source amplitude and flow velocity, the standard deviation of pressure coefficient (std Cp), see relation (6), near the bluff body is

plotted versus the flow velocity in Fig. 4. A constant value is obtained, indicating a linear relation between the force fluctuation and the square of the flow velocity.

$$Cp = \frac{p - p_{ref}}{1/2\,\rho C^2} \tag{6}$$

Hydroacoustic field

In this section, the hydroacoustic response of the circuit is analysed. The power spectral density (PSD) of pressure fluctuation at $L=0.5L_{TOT}$ is computed versus the flow velocity, in Fig. 5. Based on the linear relation (5), the source frequency is evaluated using the flow velocity. Maximum amplitude is reached at resonance as the source frequency is equal to the natural frequency (or 1st Eigen frequency) of the circuit. Similar behaviour is observed along the entire pipe. Using Eq.(5) and the value of the flow velocity inducing maximum fluctuations, it is possible to determine the 1st Eigen frequency of the circuit: fn=96 Hz.
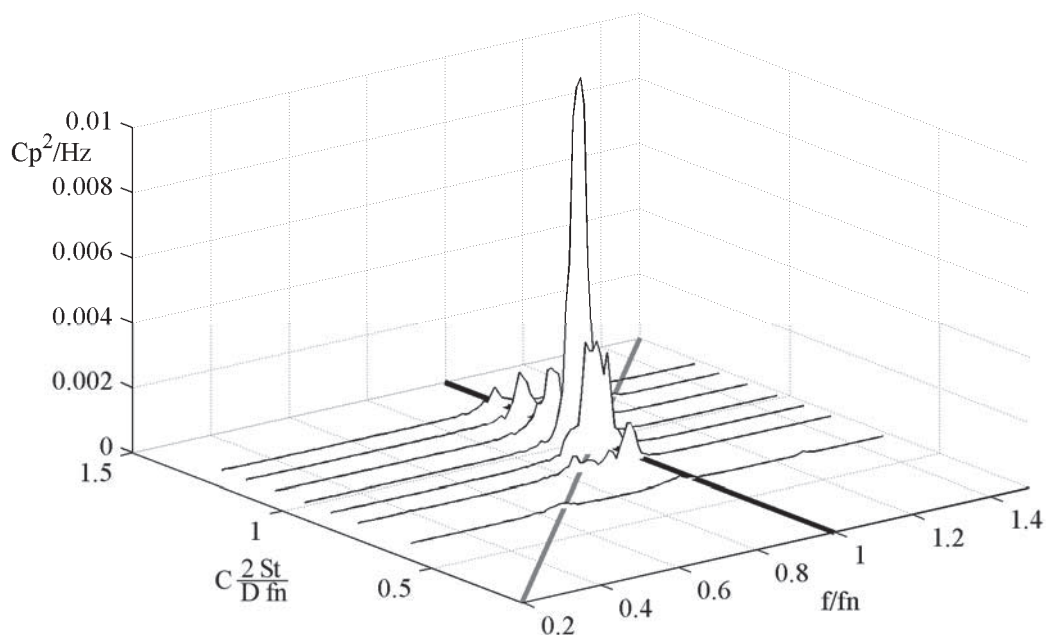

Fig. 5: PSD of the Cp at $L=0.5L_{TOT}$ versus flow velocity and equivalent source frequency. Gray line corresponds to the resulting source frequency, black line to the first Eigen frequency.

Based on the pipe length and Eigen frequency, Eq.(7), the average propagation speed in the pipe is estimated at 200 m/s.

$$2L\frac{f_k}{k} = \bar{a} \quad k = 1, 2, \ldots \tag{7}$$

This propagation speed is much slower than the velocity of sound in free water, 1485 m/s for pure water at 20° C. Nevertheless, the measured value is in good agreement with theoretical value considering the deformation of the PVC pipe wall, see [17].

4. RESULTS WITH CAVITATION

Hydrodynamic source

In the following sections, the hydrodynamic fluctuations due to the vapour cavity are analysed. For clarity, the cavitation index is normalised with the incipient cavitation index, $\sigma_i=9$. For $\sigma/\sigma_i > 1$ no vapour cavity is observed. For value lower than one, the cavity volume

increases as σ/σ_i is decreasing. Snapshots of the flow in the wake of the semi circular bluff body are presented for different σ and C= 3.8 m/s in top of

Fig. 6. The picture is taken from the top and the flow is from left to right; the field of vision is cut by a join. Based on motion detection algorithm, the cavity-water proportion in the visual field of the camera is measured; see bottom of

Fig. 6. It constitutes a good approximation of the vapour cavity volume. For $\sigma/\sigma_i = 0.86$, small cavities appear from one diameter downstream the bluff body at a location corresponding to the core of Von Karman vortices. The vapour cavities are intermittent. For $\sigma/\sigma_i = 0.64$, the presence of vapour cavity becomes permanent, but the vapour volume is continuously changing. At $\sigma/\sigma_i = 0.42$, the behaviour is similar with an increased volume. At this level of σ, cavities of considerable volume are advected beyond the scope of the camera.
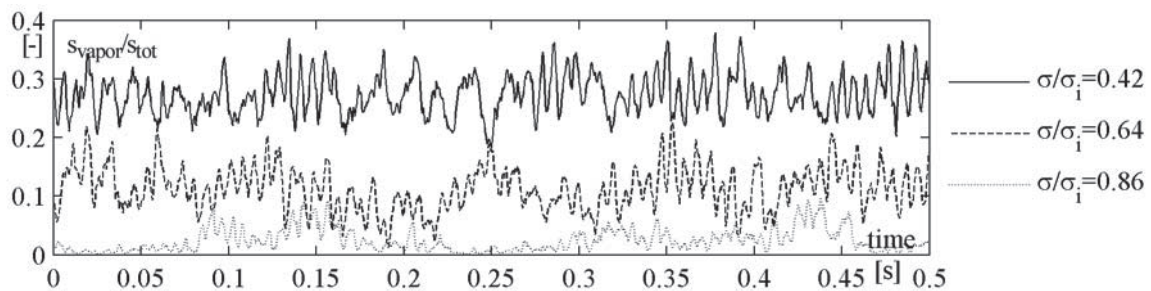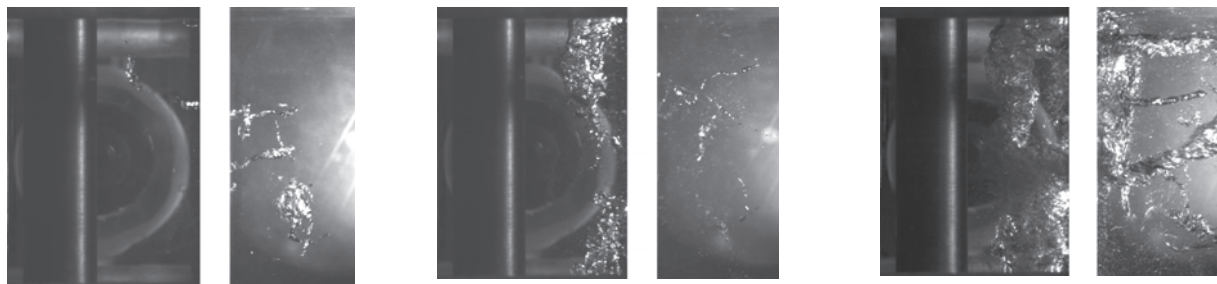
P1

Fig. 6: Top: Vortex shedding visualisation at various cavitation index with C=3.8 m/s, from left to right σ/σ$_i$=0.86, σ/σ$_i$=0.64 and σ/σ$_i$=0.42.
Bottom: Temporal evolution of vapour fraction for the corresponding σ based on motion detection algorithm.

Based on the image processing introduced previously, the frequency of vapour volume variation is determined for various C and σ, see Fig. 7. The frequency is increasing with the flow velocity but is independent of the cavitation index.
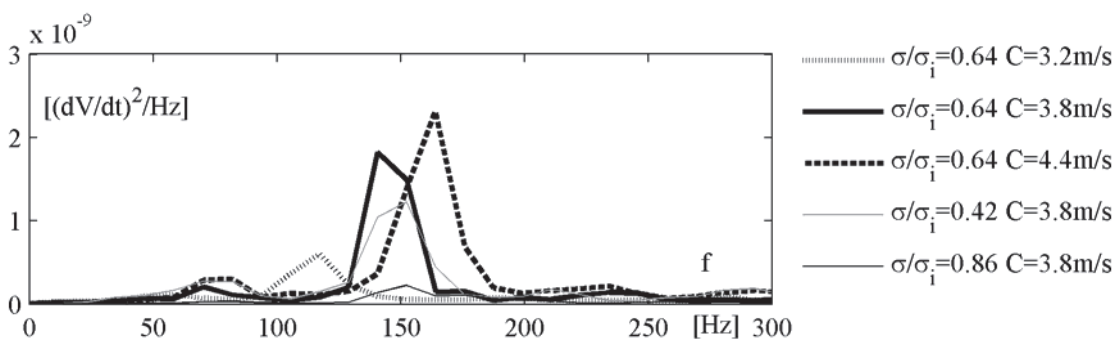

Fig. 7: Power spectral density of vapour volume fluctuation based on video images.

This vapour cavity pulsation is acting as an additional source of pressure fluctuation Eq.(8), see [7] and [13]. The variation of the cavity volume induces strong variation of average density in the wake of the bluff body. From a hydroacoustic point of view, this can be approximated as a monopole source.

$$p \approx \frac{d^2 V}{dt^2} \qquad (8)$$

From Eq.(8), pressure fluctuation at the vapour pulsation frequency is expected near the bluff body. The strength of the monopole and dipole source together is estimated using the standard deviation of the pressure coefficient near the bluff body in Fig. 8. For $\sigma / \sigma_i > 1$, the strength of the source is constant as the standard deviation near the bluff body is constant. Bellow σ_i, the vapour cavity pulsation induces additional fluctuation. The maximum source strength is reached for $\sigma / \sigma_i = 0.75$. Further decrease of the cavitations index induces a decrease of the fluctuation. This behaviour indicates a critical cavitation index which maximizes the strength of the monopole source. From the author's point of view this critical σ is specific to the experiment configuration and is independent of circuit response and eventual resonance. On the contrary, the dispersion in this range of σ is explained by the superposition of the acoustic fluctuation over the hydrodynamic fluctuation. Accordingly, the amplitude differs from normal (small amplitude) to resonant conditions (large amplitude). Nevertheless, the pressure fluctuations are amplified between 0.4 and 1 σ / σ_i independently of superimposed hydroacoustic resonance. Concerning the vortex shedding frequency, the cavitation has a weak influence. The Strouhal number is constant for most of the explored range of cavitation index. Only for very low cavitation index $\sigma / \sigma_i < 0.5$, the vortex shedding increases slightly.
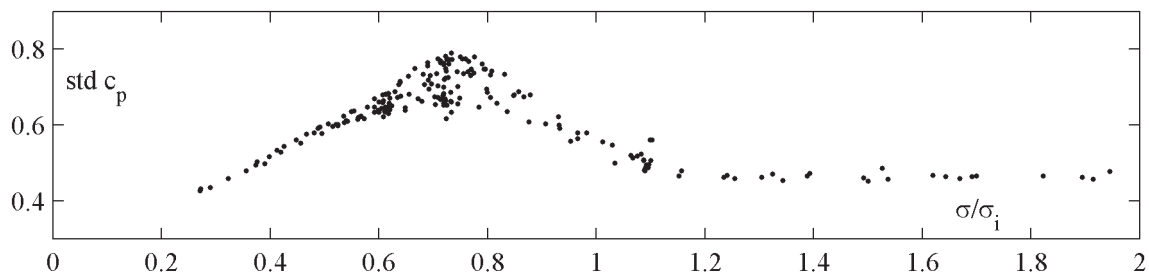

Fig. 8: Standard deviation of Cp near the bluff body versus normalised cavitation index. Black points: measured amplitude for a given σ and flow velocity.

To analyse the frequency of the source, the power spectrum of pressure fluctuation below the bluff body is computed for velocities ranging from 3 to 5.5 m/s at various cavitation indexes in Fig. 9. As shown in chapter 3, without cavitation one maximum corresponding to the vortex shedding frequency is detected. This maximum is equal to half the dipole source frequency. With cavitation, two maxima are detected. The low frequency (points) corresponds to the vortex shedding frequency and is equivalent to the case without cavitation. The high frequency (cross) is suspected to originate from the vapour cavity pulsation. Its frequency is equal to twice the vortex shedding. Accordingly the monopole and dipole source, see Eq.(5), have the same frequency. The frequency of the monopole based on linear regression of pressure measurement is in good agreement with the frequency determined from the video analysis (black dots), see Fig. 7.
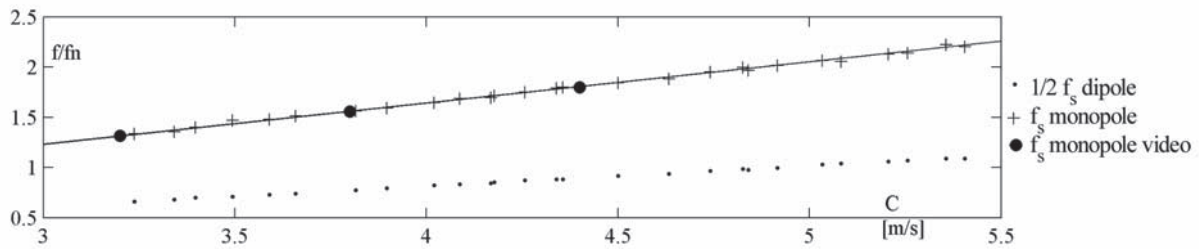
Fig. 9: Frequency of pressure fluctuation below bluff body versus flow velocity; line: linear regression of monopole frequency; black circles: vapour pulsation from video analysis.

Hydroacoustic field

In this section, the influence of the cavity compliance C_V is shown on the Eigen frequencies in Fig. 10 and mode shapes in Fig. 11. The independence of both Eigen frequency and mode shape with respect to the source frequency has been verified. In Fig.10 various flow velocity and corresponding source frequency have been used. In Fig. 11 the mode shapes are presented for a given source frequency but analogues results are obtained for different source frequency. The PSD of Cp at the middle of the pipe is plotted as a function of σ in Fig. 10. Without cavitation, the maximum amplitude induced by the broad band noise of the source corresponds to the 1st Eigen frequency. The 2nd Eigen frequency is not visible as the sensor location is close to a pressure node, see top right of Fig. 11. For $\sigma / \sigma_i < 1$, the first Eigen frequency decreases proportionally with the cavitation index. Simultaneously, the second Eigen frequency follows the same evolution. Applying Eq. 7 to the measure presented in Fig. 10, the propagation velocity in the cavitating section of the pipe is estimated in the range of 5 to 20 m/s. This estimation is obtained, assuming a variation of vapour cavity length along the pipe axis from 0 to 0.1 m, for $\sigma / \sigma_i = 1$ and $\sigma / \sigma_i = 0$ respectively. In Fig. 11, the 1st and 2nd mode shapes are presented for various σ. Points are the real part of the measured transfer function with reference sensor at L=0.5L_{TOT} and lines are spline interpolations. The increase of vapour compliance shifts the anti node of the first Eigen mode from the middle of the pipe to the vapour cavity location. Simultaneously, the central node of the second Eigen mode is shifted to the cavity location. Accordingly, the 2nd Eigen mode is detected at L=0.5L_{TOT} for $\sigma / \sigma_i < 1$, see Fig. 10.
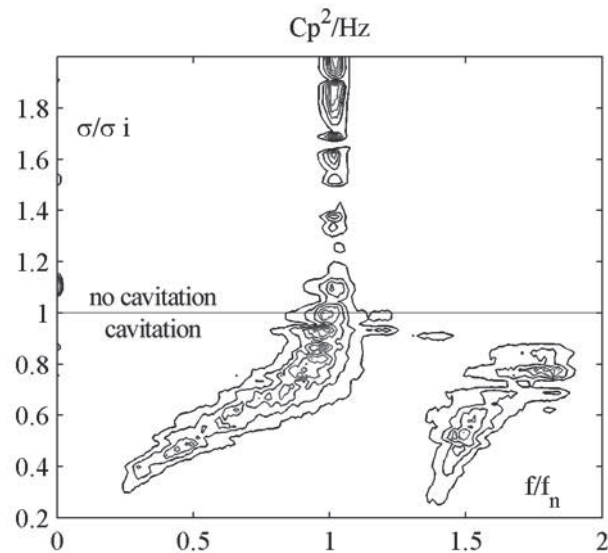
P1

Fig. 10: PSD of Cp at $L=0.5L_{TOT}$ for various σ; contour plot of isoamplitude; the dependence of the 1st and 2nd Eigen frequencies on σ is clearly visible.
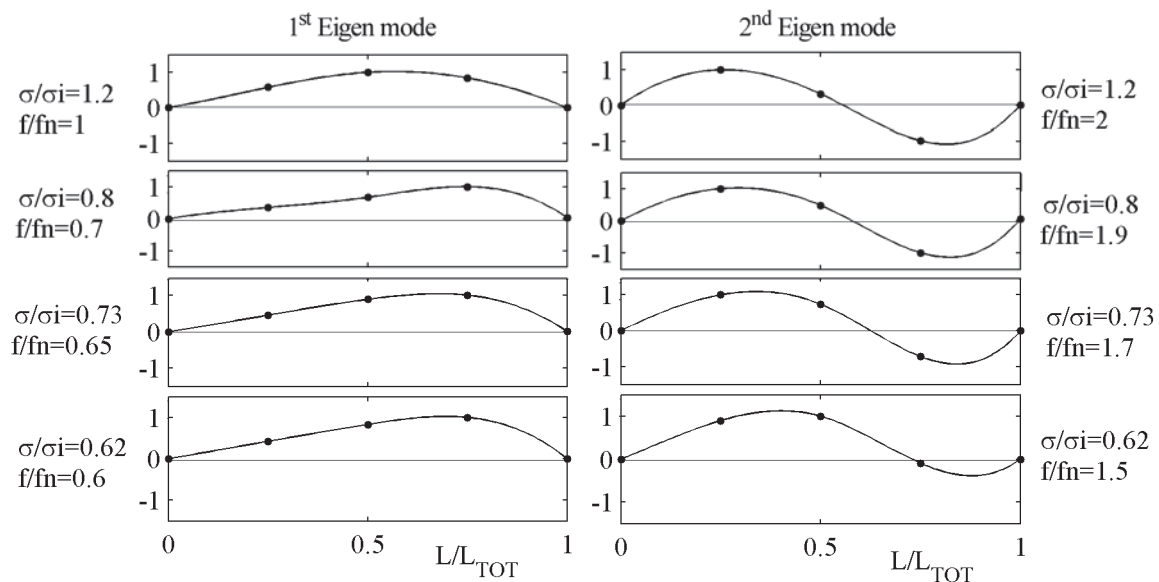

Fig. 11: 1st (left) and 2nd (right) Eigen mode shapes at various cavitation indexes; points are measured transfer function, lines are spline interpolations.

Resonance

Compared to the situation without vapour, the interaction of the hydrodynamic source with the hydroacoustic system is more complex. The Eigen frequencies and mode shapes of the system are modified by the vapour compliance. And in addition to the dipole source induced by the drag force on the bluff body, the temporal evolution of the cavity volume engenders a monopole source having the same frequency. For this reason, the hydroacoustic fluctuations are much larger with cavitation.

In Fig. 12, the PSD of Cp at the middle of the pipe is plotted versus the sources frequency for $\sigma / \sigma_i = 0.62$. Equivalent behaviour is observed along the entire pipe but the local

amplitude is determined by the mode shape, see Fig. 11. The resonant frequency is equal to 1.5 fn. It corresponds to the 2nd Eigen mode.
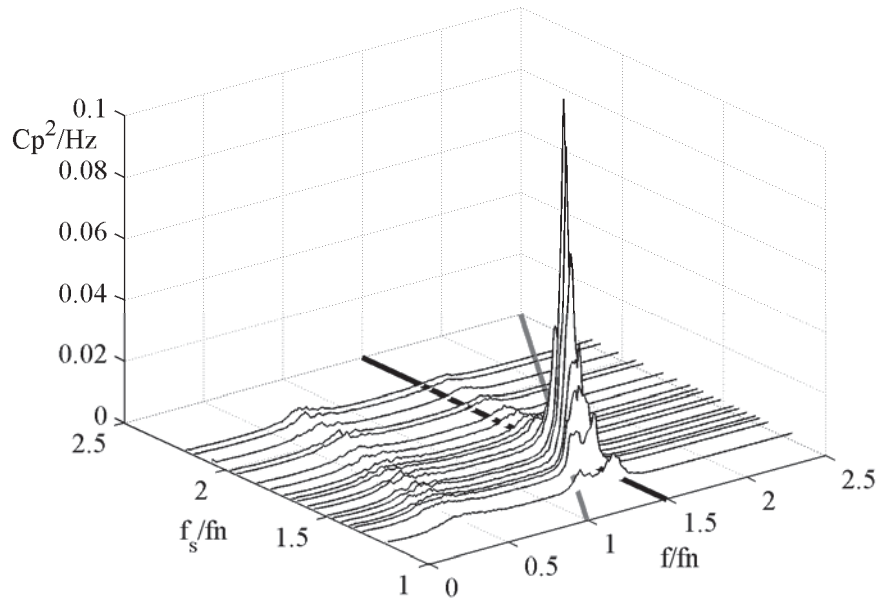
Fig. 12: PSD of the Cp at L=0.5L$_{TOT}$ for different flow velocities and resulting source frequencies at σ/σ$_i$=0.62. Gray line corresponds to the sources frequency, black line to the Eigen frequency.

As shown in the previous section, the intensity of the sources depends on the cavitation index. For this reason, the resonant amplitude is also strongly influenced by σ. In Fig. 13, the standard deviation of the pressure fluctuation at the middle of the pipe is plotted versus the cavitation index and source frequency. Bellow σ$_i$, the resonant frequency is decreasing with σ meanwhile the resonant amplitude is strongly influenced by σ. The maximum amplitude, std Cp=0.98, is reached for $\sigma / \sigma_i = 0.62$ with sources frequency equal to 1.5 fn. The fluctuations amplitudes are much higher than for the case without cavitation; the maximum standard deviation of Cp is nearly 5 times higher.
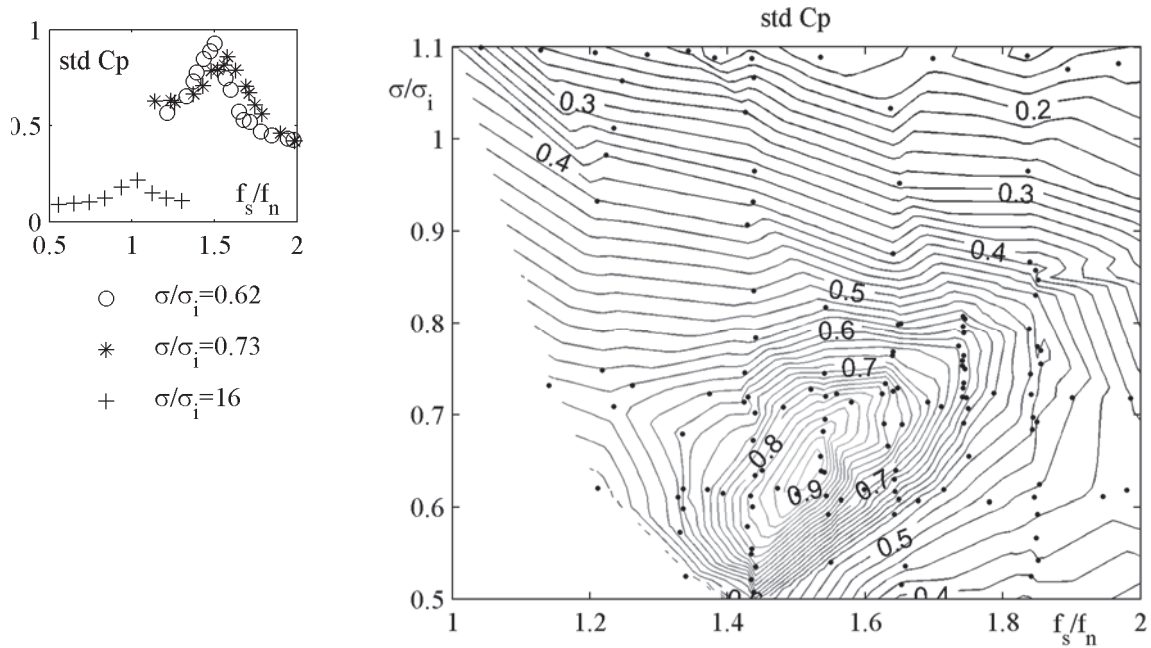
Fig. 13: Standard deviation of Cp versus source frequency and σ. Right: isoamplitude contour plot based on linear interpolation; points are measured flow conditions. Left vertical cut at constant σ.

5. CONCLUSION

The influence of cavitation on hydroacoustic resonance in pipe has been studied. Two major effects of vapour cavity were observed:

- First, the Eigen frequency of the pipe is decreased by the vapour cavity. Bellow σ_i, the Eigen frequencies decrease with σ.
- Second, the fluctuation of cavity volume in the wake of the bluff body is acting as an additional source of pressure fluctuation. The resulting monopole source has the same frequency as the dipole source induced by the drag force.

Consequently, the resonance frequency and amplitude is dependent on the cavitation index. And in the present experiment, the maximum amplitude of pressure fluctuation at resonance was obtained with an intermediate cavitation level. At this cavitation level, amplitudes were up to 5 times higher than for the case without cavitation. The results of the present experimental investigation put into the light the importance of the vapour cavity dynamic in the study of hydroacoustic systems.

6. ACKNOWLEDGEMENTS

7. REFERENCES

[1] Rheingans, W. J.: Power Swing in Hydroelectric Power Plants, *Transaction ASME 62, pp. 171-184*

[2] Lighthill M. J.: On Sound Generated Aerodynamically. I. General Theory. *Proceedings of the Royal Society of London. Series A, Vol. 211, No. 1107, pp. 564-587, 1952*

[3] Ffowcs Williams, J. E., Hawkings, D. L.: Sound Generation by Turbulence and Surfaces in Arbitrary Motion. *Philosophical Transactions of the Royal Society of London. Series A, Vol. 264, No. 1151, pp. 321-342, 1969*

[4] Ffowcs Williams, J. E.: Hydrodynamic Noise, *Annual Review of Fluid Mechanics, Vol 1, pp.197-222, 1969*

[5] Reethof, G.: Turbulence Generated Noise in Pipe Flow, *Annual Review of Fluid Mechanics, Vol 10, pp.333-367, 1978*

[6] Dorfler, P.: System Dynamics of the Francis Turbine Half Load Surge. *11th symposium IAHR, Amsterdam. Vol.2: Proceedings, 1982*

[7] Duttweiler, M. E., Brennen, C. E.: Surge Instability on a Cavitating Propeller. *J. Fluid Mech.,Vol. 458, pp. 133-152, 2002*

[8] Nicolet, C.: Hydroacoustic Modeling and Numerical Simulation of Unsteady Operation of Hydroelectric Systems, *PhD thesis EPFL, 2007*

[9] Arpe, J., Nicolet, C., Avellan, F.: Experimental Evidence of Hydroacoustic Pressure Waves in a Francis Turbine Elbow Draft Tube for Low Discharge Conditions, *Journal of Fluids Engineering, Vol. 131, Issue 8, 2009*

[10] Rienstra, S.W., Hirschberg, A.: an Introduction to Acoustics. *Eindhoven University of Technology, 2008*

[11] Berger, E., Wille, R.: Periodic Flow Phenomena, *Annual Review of Fluid Mechanics, Vol. 4, pp. 313-340, 1972*

[12] Williamson, C. H. K.: Vortex Dynamics in the   Cylinder Wake, *Annual Review of Fluid Mechanics, Vol 28, pp.477-539, 1996*

[13] Villouvier, V.: Modeling of Hydroacoustic Sources of Butterfly Valves, *Forum Acousticum, Budapest, 2005*.

[14] Ota, T., Okamoto, Y., Yoshikawa, H.: A Correction Formula for Wall Effects on Unsteady Forces of Two-Dimensional Bluff Bodies, *Journal of Fluids Engineering, Vol. 116 pp. 415-418, 1994*

P1

[15] Farhat, M., Natal, S., Avellan, F., Paquet, F., Lowys, PY., Couston, M.: Onboard Measurments of Pressure and Strain Fluctuations in a Model of Low Head Francis Turbine, Part 1:Instrumentation. *AIRH Symposium, Lausanne, 2002*

[16] Inoue, O., Hatakeyama, N.: Sound Generation by a Two-Dimensional Circular Cylinder in a Uniform Flow. *Journal of Fluid Mechanics, Vol. 471, pp.285-314, 2002*

[17] Dwynn Lafleur, L., Douglas Shields, F.: Low-Frequency Propagation Modes in a Liquid-Filled Elastic Tube Waveguide. *J. Acoust. Soc. Am., Vol 97 (3), pp. 1435-1445, 1995.*

8. NOMENCLATURE

a	$(m.s^{-1})$	propagation velocity
C	$(m.s^{-1})$	flow velocity
Cp	(-)	pressure coefficient
C_V	$(m.s^2)$	compliance
D	(m)	bluff body diameter
f	(Hz)	frequency
f_s	(Hz)	source frequency
f_{lift}	(Hz)	lift force frequency
f_{drag}	(Hz)	drag force frequency
f_k	(Hz)	Eigen frequency
fn	(Hz)	natural or 1st Eigen frequency
L_{TOT}	(m)	pipe length
p	(Pa)	pressure
p_v	(Pa)	vaporisation pressure
p_{ref}	(Pa)	downstream reservoir pressure
s	(m^2)	surface
V	(m^3)	vapour volume
σ	(-)	cavitation index
σ_i	(-)	incipient cavitation
ρ	$(kg.m^{-3})$	water density
Std	(-)	standard deviation
PSD	(-)	power spectral density